論文 Seismic Behavior of Beams of Reinforced Concrete Highway Frame Structure

Wael ZATAR *1, Hiroshi MUTSUYOSHI *2, Yoshito KONISHI *3
and Atsushi MORI *4

ABSTRACT: After retrofitting of RC piers of an elevated π-shaped expressway, a subsequent assessment of the overall double column bents left doubts that some of the un-retrofitted parts might experience undesirable failures that might prohibit achieving the target ductility. Consequently, an experimental program, where quantity of shear reinforcement of RC beams was the experimental variable, was conducted. Furthermore, a numerical analysis was performed to check applicability of the finite element technique. Overall behavior, damage propagation, failure mechanism and modes were investigated. Appropriate strengthening for the RC beams should be employed to ensure better performance during future earthquakes.
KEYWORDS: Earthquake resistant structures, shear capacity, reversed cyclic loading, shear enhancement, seismic strengthening, numerical analysis.

1. INTRODUCTION

Tremendous damages to bridges in general and to piers in particular were a direct result of the disastrous Hyogo-Ken Nanbu 1995 earthquake in Japan. Many bridges were collapsed due to lack of ductility [1]. Such a catastrophic event led to avenues for questions and research on seismic behavior and possible rehabilitation and/or strengthening of RC structures and specifically bridges not only in Japan but worldwide as well. Due to the disastrous event, many RC bridge piers had experienced severe damage and many of them have been strengthened by the use of steel or concrete jacketing as reported by Kawashima [2] and also elsewhere [3,4,5].
The operational authority supervising an elevated RC expressway that was constructed in 1972 carried out a necessary preliminary assessment of the double column bents of the expressway to sustain future natural disasters. Such expressway's system is known in Japan as elevated RC π-shaped viaduct structures. It was found that the RC piers lack sufficient ductility because of inadequate shear reinforcement. Since a more reliance should be placed on achieving ductile members in bridge structures [6], a retrofitting technique for the RC piers by the use of steel jacketing was employed in response to the first phase of the expressway assessment. Nevertheless, a subsequent assessment of the overall as-built double column bents incorporating the retrofitted piers left doubts that the un-strengthened parts including RC beams and beams to piers connections might experience undesirable failures that might prohibit achieving the overall target ductility of the bents during future earthquakes. Consequently, it was decided to conduct an experimental investigation in the form of a program that consisted of two small-scaled models to ascertain the overall behavior, damage propagation, failure mechanism and modes of failure. The employed quantity of shear reinforcement of the RC beams was the experimental variable herein. Furthermore, a numerical analysis was then performed to check and/or confirm the applicability of the finite element technique to simulate the overall double bent response and behavior. Finally, recommendations to ensure better performance of the bents during future events were proposed.

*1 Department of civil and Environmental Engineering, Saitama University, Dr. Eng., Member of JCI
*2 Department of civil and Environmental Engineering, Saitama University, Prof. Dr., Member of JCI
*3 Metropolitan Expressway Public Corporation, Tokyo, Japan
*4 Japan Engineering Consultants Co. Ltd., Tokyo, Japan

2. EXPERIMENTAL PROGRAM

Results of two small-scaled specimens (named SP1 and SP2) that represent 1/7-scaled actual double column bents are presented herein. Main experimental variable was the quantity of shear reinforcement of the RC beams while all details of the other parts of the specimens were identical. Each specimen consisted of a footing, two identical columns and a beam. Footing dimensions were 450 x 600 x 2250 mm. Column dimensions were 300 x 300 x 1300 mm while those of the beam were 240 x 300 x 2350 mm. Analytical investigations declared that it was not expected that the retrofitted columns of the double column bents' prototypes would experience major damages because of the retrofitting effect of the steel jacketing. To simulate the retrofitted columns in the specimens level, columns with an adequate percentage of shear reinforcement (0.38%) were utilized. Strength ratios between the beam and the columns were chosen to represent the actual ones. The shear reinforcement of SP1 was chosen to represent the least critical quantity (0.05%) found in the as-built cases while that of SP2 was chosen to represent the average of many actual cases with comparatively low shear reinforcement ratios (0.1%). Rapid hardening concrete with a cylinder compressive strength of 36.4 MPa and a max aggregate size of 20 mm was utilized. Properties of the reinforcing bars are shown in Table 1 while the information concerning specimen details are illustrated in Fig. 1.

Table 1: Properties of rebars

Reinforcing Bars	Yield Strength (MPa)	Yield Strain (μ)
D3	340	2070
D10	415	2600
D13	417	2340
D16	413	2870

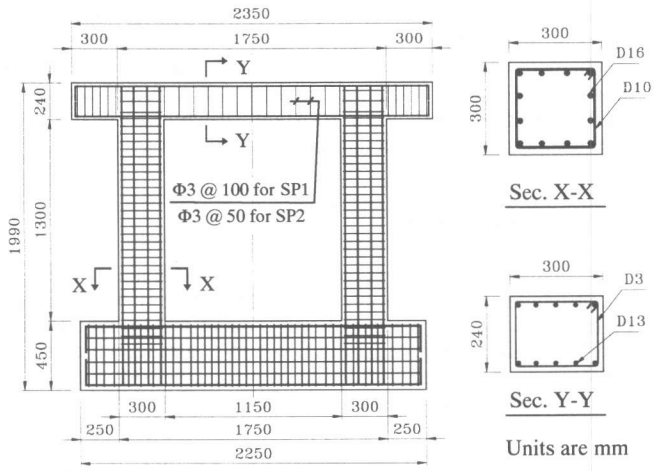

Fig. 1: Specimen details

3. LOADING SETUP AND INSTRUMENTATION

Specimens were tested under reversed cyclic loading in the test frame illustrated in Figure 2. An actuator, of a 500 kN capacity and a maximum stroke of ±100 mm, fixed horizontally to a loading frame, was connected to the specimens at level of the beams. Additionally, simulated main working loads on the superstructure were applied to the specimens through imposing a vertical load of 106 kN at the top of the beams at their mid-spans.

Specimens were subjected to pre-determined displacement excursions. First displacement amplitudes were ±2.5 mm followed by displacement amplitudes of ±5 mm. Then the specimens were subjected to sequentially increasing multiple integers of yielding displacements. The yield displacement (δ_y) was defined as the lateral deflection corresponding to attaining estimated yield load (P_y) of the reinforcing bars. Three repetitions of each cycle were utilized during testing. Ultimate displacement was defined as the displacement corresponding to 80% of the maximum load in the post-peak region obtained in the skeleton (backbone) curve.

Concrete and steel strains at various locations, deflections along the beam lengths, axial & lateral displacements and strains were monitored during each test through the use of an extensive instrumentation. Longitudinal concrete strains were measured by using Linear Voltage Displacement Transducers (*LVDTs*) over gauge lengths of 50 ~ 100 mm. Also mold gauges that

are known in Japan as rosette gauges were used on the beams surfaces to record multi-directional strains during testing. Strain gauges were allocated on surfaces of the reinforcing bars in the expected plastic hinge regions of the columns and at different locations along the beam length. Data logger, A/D converter, D/A converter, actuator controller, hydraulic jack, pump, load-cells and a personal computer to control input/output data were employed during testing.

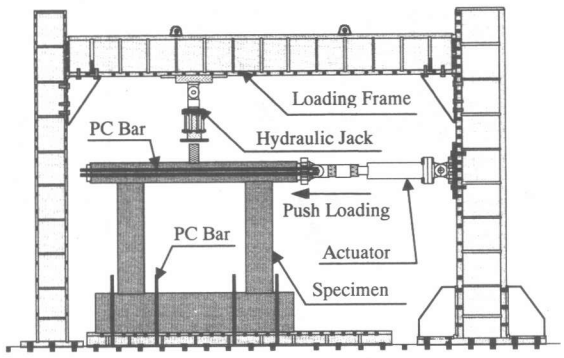

Fig. 2: Experimental loading setup

4. TEST RESULTS & DISCUSSION

Behavior of each specimen is illustrated graphically in the form of hysteretic load versus displacement relationship. Displacements were determined from readings of an upper *LVDT* located at the same level of both the loading actuator and the beam. Final failure modes and their associated mechanisms were also observed. Yielding of the reinforcing bars at various expected plastic hinge locations were marked on the hysteretic load-displacement relationship.

Fig. 3 shows the hysteretic load-displacement curve of specimen SP1. Yielding of the longitudinal bars at the lower plastic hinges of both columns (positions B, A) was observed when the transducer allocated at the actuator's level recorded displacement ductilities of δ_y and $-\delta_y$, respectively. At this loading stage, some flexural cracks were formed in the beam and another cracks were initiated in the bottom plastic hinges of the columns. Additionally, shear cracks were observed only at both sides of the beam together with X-shaped cracking in the beam-to-column connections. During the push loading at a displacement of about $+1.25\delta_y$, yielding of the bottom reinforcing bars of the beam's right plastic hinge (position F) was recorded followed by yielding of the top reinforcing bars of the beam's left plastic hinge (position E) at a displacement ductility of about $+1.95\delta_y$. Shear cracks were very obvious with noticeable widths. When loading in the other direction (pull loading) till a displacement ductility of $-\delta_y$, a major shear crack responsible for the specimen failure was observed after which a sudden reduction in the load was recorded.

Fig. 4 shows the hysteretic load-displacement curve of specimen SP2. Yielding of the longitudinal bars at the lower plastic hinge of the right column (positions B) was observed when the transducer allocated at the actuator's level recorded a displacement ductility of δ_y. similar to specimen SP1, some flexural cracks were formed in the beam and another cracks were initiated in the columns' lower plastic hinges. Additionally, shear cracks were observed at both sides of the beam accompanied by X-shaped cracking in the beam-to-column connections. During the push loading at a displacement of about $+1.2\delta_y$, yielding of the longitudinal bars at the lower plastic hinge of the left column (positions A) was observed. Then, yielding of the bottom reinforcing bars of the beam's right plastic hinge (position F) was observed at a displacement ductility of $+1.6\delta_y$ followed by yielding of the top reinforcing bars of the left plastic hinge of the beam (position E) at a displacement ductility of about $+1.9\delta_y$. Shear cracks were obvious with noticeable widths at $\pm 2\delta_y$. Continuing loading until $\pm 3\delta_y$ showed that the previous flexural cracks number was increased and widths of the major shear cracks were greatly increased. When loading in the push direction to $+4\delta_y$. Shear failure occurred in the left side of the beam. For both specimens, neither of the reinforcing bars at the expected plastic hinges at top of the columns experienced yielding. Although it was clear that the behavior of SP2 is better than that of SP1 because of the increased shear reinforcement ratio, it can be clearly pointed out that only for the tested specimens since the retrofitted columns have adequate ductility, the beams of the such expressway may require additional strengthening to allow achieving the desired overall structural displacement ductility. To confirm generalization of this conclusion, additional analytical study was conducted for the as built double column bents for a wide range of relative flexural to shear strengths between the beams and the columns. Because of space limitations, the analytical results will not appear in this document. Indeed, it should be noted that the concluded remarks are solely based on the experimental investigation, which did not encounter possible effect of deck slab and secondary beams of the superstructure on the overall structural behavior that is now taken care of in a current study.

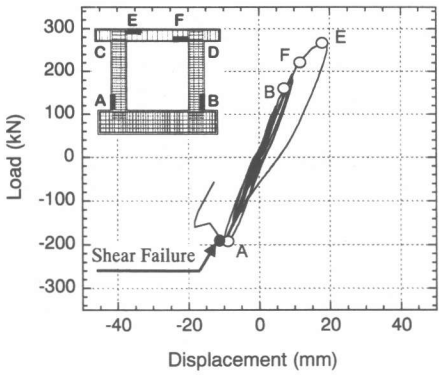

Fig. 3: Load-displacement curve of SP1

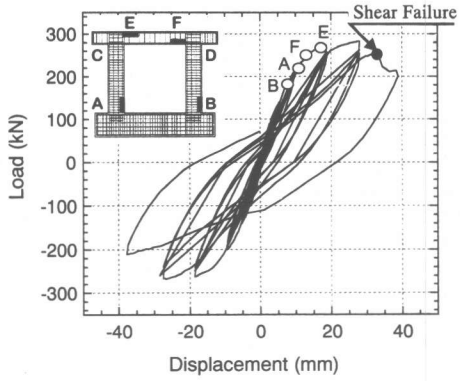

Fig. 4: Load-displacement curve of SP2

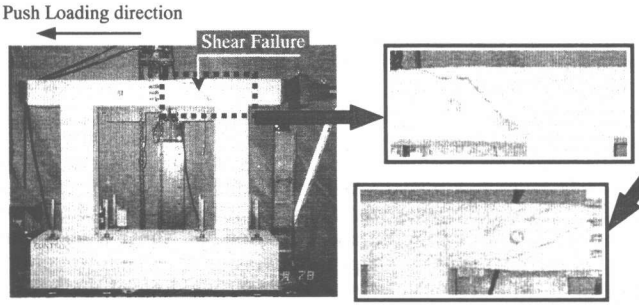

Fig. 5: Photo of final failure mode of SP1

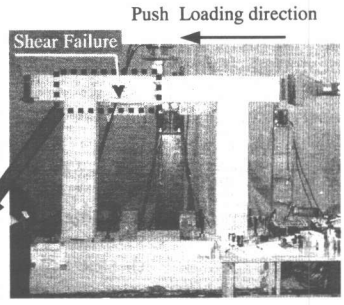

Fig. 6: Photo of final failure mode of SP2

During the push loading, the adjacent right beam-to-column connection was an opening moment connection while the left one was a closing moment connection. It can be observed that failure of SP1 was in the beam's right part during the pull loading (closing moment connection) while failure of SP2 was in the beam's left part during the push loading (closing moment connection). This can be attributed to the fact that the critical shear force was originated near the closing moment connections of both specimens since gravity and seismic shear moments are additive while these moments oppose each other in the case of opening moment connections.

For the case of closing moment connections, fan-shaped patterns were developed radiating from the outer surfaces of the beam and the column toward the inside corner. This pattern can be modeled as a diagonal strut.

For the case of opening moment connections, anchorage of the column bars closest to the beam was provided by two struts. The first strut (S1) was directed toward the column compression resultant while the second one (S2) was directed outward into the beam. Vertical component of the second strut was carried by the beam stirrups close to the joint. Transfer of this tensile forces to the top of the beam provided the necessary force to incline the beam upper compression force into the major compression strut (S3).

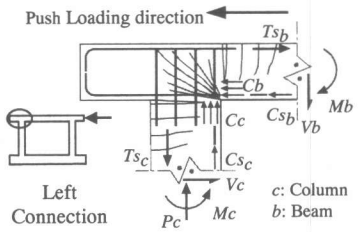

a) Closing moment connection

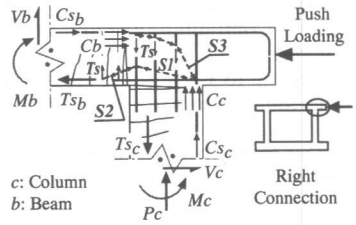

b) Opening moment connection

Fig. 7: Closing and opening moment connections

5. OUTLINE OF NUMERICAL MODELING

To simulate the behavior of the experimental specimens of the double column bents, a non-linear FEM approach was adopted. A plain stress analysis was carried out under displacement control scheme up to ultimate state with the aid of WCOMD program [7].

5.1 FINITE ELEMENT MESH AND MATERIAL MODELING

A decision of using eight-noded parabolic isoparametric elements to model the double column bent elements was taken after a preliminary mesh sensitivity analysis. Both RC and plain elements were used herein to characterize the concrete behavior near and away from the reinforcing bars [8,9]. Elastic elements were used at the ends and over the mid part of the beam to simulate the steel plates at which the actuator and the hydraulic jack appliy their loads while joint elements were employed to simulate the columns-to-footings interface joints. A total of 203 RC, 19 plain, 7 elastic and 6 joint elements were utilized in the analysis (Fig. 8).

The employed RC plate elements [7] deal macroscopically with cracks and reinforcing bars by modeling the relationship between average stress and average strain. Principal of superposition was adopted in computation of elements' stiffness matrices. Formulation of the RC elements was adopted through combining constitutive law of cracked concrete and that of reinforcing bars where the constitutive law of cracked concrete considers tension stiffening, compression and shear transfer models. Experimental material properties were used. Based on Shawky and Maekawa [10], the following failure criteria were adopted.

- Tension failure: when tensile strain perpendicular to crack reaches a maximum value of 3%.
- Compression failure: when compressive strain parallel to crack reaches a maximum value of 1%.
- Shear failure: when shear strain along a crack plane reaches a maximum value of 2%.

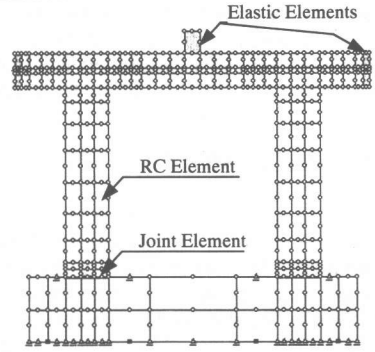

Fig. 8: Analytical FE mesh

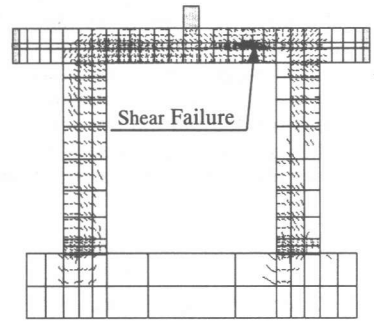

Fig. 9: Analytical cracking and failure of specimen SP2

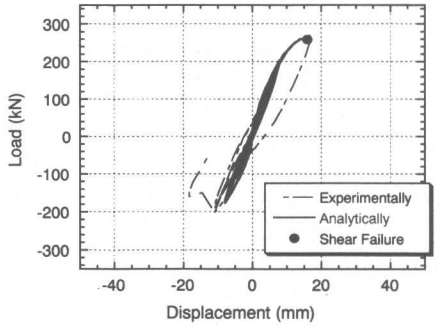

Fig. 10: Analytical and experimental Load-displacement curves of SP1

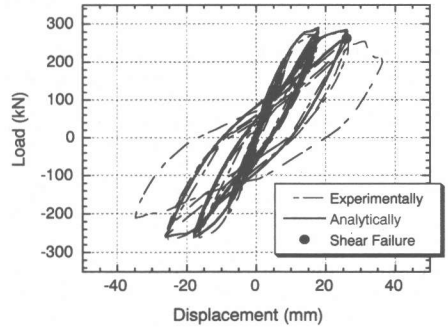

Fig. 11: Analytical and experimental Load-displacement curves of SP2

5.2 NUMERICAL RESULTS AND COMPARISONS

Numerical hysteretic load-displacement relationships, maximum and ultimate failure loads, cracking patterns and final failure modes were compared with the previously obtained

experimental results. Because of space limitations, an example of the cracking pattern is presented herein as shown in Fig. 9 for SP2 where shear failure was observed. Fig. 10 shows the hysteretic behavior of SP1 where it can be observed that shear failure was obtained at a displacement ductility of $+2\delta_y$. Although the predicted shear failure was in the push loading direction while that observed experimentally was in the pull direction, the predicted failure load and displacement were efficiently predicted numerically. Fig. 11 shows the hysteretic behavior of SP2 where shear failure was observed at a displacement ductility of $+3\delta_y$ while the experimental one was at a displacement ductility of $+4\delta_y$. Both of the shear failures predicted analytically and obtained experimentally were in the push direction, In general, the numerical FE simulation of both specimens shows that it can be effectively employed to simulate the behavior of the concerned double column bents in condition that appropriate mesh, material modeling and element type are utilized.

6. CONCLUSIONS

Assessment of the overall double column bents of an existing retrofitted highway left doubts that some of the un-strengthened parts may experience undesirable failures that might prohibit achieving the target ductility during future earthquakes. Consequently, an experimental program was conducted incorporating high ductile columns that can simulate the retrofitting effect of the columns. Furthermore, a numerical analysis was performed to check the applicability of the finite element technique. Through investigation of damage propagation, failure mechanism and overall hysteretic behavior of the specimens, the following conclusions were drawn:

1. The expected upper plastic hinges of the simulated retrofitted columns have adequate strength that ensured minimal damages. The expected lower plastic hinges have enough strength and ductility since their recorded damages were not severe. On the other hand, the beams suffered considerable damages and failed in a shear mode at comparatively low ductilities.
2. Appropriate strengthening for some RC beams may be employed to ensure a better overall performance and full use of the high ductile columns.
3. The numerical simulation verified the effectiveness of employing FEM to simulate the behavior in condition that appropriate mesh, material modeling and element type are employed.

ACKNOWLEDGMENT

Special thanks are due to Mr. H. Koizumi and the members of Structural Material Lab. of Saitama University who assist during conducting the experimental program.

REFERENCES

1. WG Special JSCE Committee Report for the Hansion-Awaji Earthquake Disaster, "Damage Analysis and Ductility Evaluation Plan of the Hansion-Awaji Earthquake Disaster,".
2. Kawashima, K., "Seismic Design and Retrofit of Bridges," 12th World Conference of Earthquake Engineering (WCEE), A State of The Art Report, 2000, Paper No. 2828.
3. Takahashi, H., Mutsuyoshi, H. and Kondo, E., "Seismic Behavior of Strengthened RC Beams," Proc. of JCI, Vol.18 (2), 1996, pp.1493-1498 (In Japanese).
4. Tobuchi, S., Kobayashi, M., Thuyoshi, T. and Ishibashi, T., "Reversed Cyclic Tests of RC Piers Strengthened by External Rods," Proc. of JCI, Vol.21 (3), 1999, pp.1333-1338 (In Japanese).
5. Kamogawa, S., Yamakawa, T. and Kurashige, M., "Seismic Tests of RC Piers Strengthened by PC Tendons," Proc. of JCI, Vol.21 (1), 1999, pp.415-420 (In Japanese).
6. Priestley, M. J. N., "Design of Single Level Bridges for Joint Shear," Structural Systems Research Report SSRP 93/02, University of California, San Diego, Feb. 1993.
7. Okamura, H. and Maekawa, K., "Nonlinear Analysis and Constitutive Models of Reinforced Concrete," Gihodo Press, Tokyo, 1991.
8. Xuehui, A., Maekawa, K. and Okamura, H., "Numerical Simulation of Size Effect in Shear Strength of RC Beams," J. of Mat., Conc. Struct. and Pav., JSCE, Vol.35, No.564, 1997, pp.297-316.
9. Maekawa, K., Xuehui, A. and Tsuchiya, T., "Application to Failure Analysis of Reinforced Concrete Structures," Concrete Journal published by JCI, Vol.37, No.9, Sep 1999, pp.54-60.
10. Shawky, A. and Maekawa, K., "Nonlinear Response of Underground RC Structures under Shear," J. of Mat., Conc. Struct. and Pav., JSCE, Vol.31, No.538, 1996, pp.192-206.